TOPOLOGY OPTIMIZATION OF MASS UNDER MULTIPLE LOAD CONDITIONS AND MATERIAL FAILURE CONSTRAINTS

Eduardo A. Fancello
GRANTE, Departamento de Engenharia Mecânica, Universidade Federal de Santa Catarina - Brasil.
e-mail: fancello@grante.ufsc.br

Jucelio T. Pereira
Departamento de Engenharia Mecânica, Centro Federal de Educação Tecnológica do Paraná - Brasil.
e-mail: jucelio@cefetpr.br

Abstract: *This work presents a numerical approach to deal with the topology optimization of a mechanical device in which the minimum mass is searched subject to material failure constraints and multiple load conditions. The formulation combines the SIMP approach and the Augmented Lagrangian technique in order to handle local stress constraints. The consideration of multiple loads in this formulation follows as a simple extension of the single loaded case. Analyitical sensitivity analysis is used to obtain low costs derivatives. Three numerical results are presented in order to compare final designs due to each load case and due to the multiple loaded case. An important observation is that the final design due to a multiple loaded case is not a simple envelope of a single loaded case. Morover, the numerical costs of considering multiple loads are not much greater than those of the single loaded case.*

Key words: Structural optimization, topology optimization, multiple load conditions, material failure constraints.

1 Introduction

The design of mechanical devices that use the least material as possible but are capable of performing their function without material failure is an attractive and frequent goal in industrial applications. Topological optimization is perhaps today's most flexible numerical tool available to perform a systematic search of this kind of designs. The literature associated with this research area show several approaches to solve this problem and, despite not being rigorous, two groups of techniques may be distinguished.

The first one contains those formulations in which a classical optimization problem is set and its solution obtained through mathematical programming techniques. The second group includes those approaches that define a local criterion to update the design variables. This criterion may be related to optimality conditions or being an heuristic construction. Moreover, it is called local if the design change at a particular material point depends on information of just a neighborhood of that point.

Both approaches have several advantages and drawbacks. Formulations from the first group hold a clear mathematical structure and their solution guarantee the satisfaction of the optimization statement. They are also quite flexible in the sense of being capable to consider different types of constraints and cost functions. The prize of these benefits is the computational cost of solving a mathematical programming problem in which the evaluation of cost function, constraints and their derivatives involves the solution of equilibrium equations. Moreover, convergence problems are usually faced.

Algorithms from the second group usually spend much less time of CPU than those from the first group. They do not usually show convergence problems, in many cases for the simple reason that no convergence test is applied besides some care about instable design evolutions. In spite of these advantages, the final design has no commitment to satisfy the original desired requirements.

Only a few works dealing with mass minimization and material failure constraints in continuum structures may be found within the first approach. Among them, Duysinx & Bendsøe (1998), Duysinx & Sigmund (1998), Stolpe & Svanberg (2001), Pereira (2001) Pereira et al. (2003) The second approach has received increasing attention, mainly due to their simplicity and relative low computational effort. Fully stressed based algorithms, evolutionary algorithms, performance based algorithms, etc., should be classified within the second group. Among many others, Xie & Steven (1993,1997), Cursi & Pagnaco (1995) , Novotny et al. (1998) , Querin et all (2000), Lin & Chao (2001) .

The present work is based on the first approach and addresses the most frequent situation on mechanical design: multiple load conditions.

Multiple load conditions are usually treated as a multiobjective optimization in the compliance problem; the objective function is a weighted combination of the compliances of each load condition. However, difficulties arises by the time of defining the value of the corresponding weights. In evolutionary or fully-stressed type algorithms, multiple loads are frequently treated by including some heuristics in the local criterion in order to take into account the mechanical response due to each load. On the other hand, the mathematical problem of mass minimization subject to local material failure constraints and multiple load cases is just a natural extension of that with a single load case. No additional heuristic or weighting function definition is needed. Moreover, it will be seen that numerical

costs associated with of a multiple loaded problem are not necessarily much greater than those of a single loaded case.

This paper should be viewed as an extension of the work of Pereira et all (2003) in order to include multiple load conditions.

For a given domain Ω, the problem to be solved is

$$\begin{array}{ll} \text{Minimize} & \text{Mass} \\ \text{Subject to :} & F_i\left(\sigma_i\left(\mathbf{x}\right)\right) \leq 0, \quad \forall \ \mathbf{x} \in \Omega, \quad i = 1...N, \end{array} \tag{1}$$

where F_i is a material failure function related to the stress field $\sigma_i\left(\mathbf{x}\right)$ in equilibrium with the corresponding i-th load case. N is the number of load cases. It is well known that direct treatment of (1) as a problem of finding a characteristic function indicating existence or not-existence of material is ill-posed. Therefore, several techniques are used to circumvent this problem. The present work formulates (1) in the same way as developed in Duysinx & Bendsøe (1998), i.e. combining the SIMP technique and a local material failure constraint. The numerical approach, however is quite different. The next three sections are dedicated to present briefly the principles of the formulation and its numerical approach. Section 5 presents numerical examples in which optimal designs for multiple loaded structures are analyzed.

2 Formulation

For simplicity sake the state equations are restricted to linear elastic elasticity where a body Ω submitted to contact forces $\bar{\mathbf{t}}$ and known displacements $\bar{\mathbf{u}}$ on its boundary as shown in Figure 1. As in most topological problems, we distinguish the material part Ω_m of Ω and the void region Ω_v. Being $\mathbf{u}, \varepsilon(\mathbf{u})$ and $\sigma(\mathbf{u})$ the displacement, strain and stress fields and $\mathbf{D}$ the elasticity tensor, we have the following boundary value problem:

$$\begin{aligned} \sigma(\mathbf{u}) = \mathbf{D}\varepsilon(\mathbf{u}) &= \mathbf{D}\nabla^{\mathbf{S}}\mathbf{u} \ , \\ \text{div } \sigma(\mathbf{u}) &= \mathbf{0} \qquad \forall\, \mathbf{x} \in \Omega \ , \\ \sigma\ \mathbf{n} &= \bar{\mathbf{t}} \qquad \forall\, \mathbf{x} \in \partial\Omega_N \subset (\partial\Omega_m \cap \partial\Omega) \ , \\ \sigma\ \mathbf{n} &= \mathbf{0} \qquad \forall\, \mathbf{x} \in \partial\Omega_F := \partial\Omega_m \backslash (\partial\Omega_N \cup \partial\Omega_D) \ , \\ \mathbf{u} &= \bar{\mathbf{u}} \qquad \forall\, \mathbf{x} \in \partial\Omega_D \subset (\partial\Omega_m \cap \partial\Omega) \ . \end{aligned} \tag{2}$$

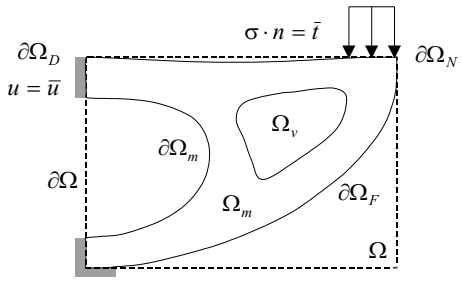

Figure 1: Geometric definitions of a domain composed by solid and voids.

Using the SIMP artificial microstructure (Solid Isotropic Microstructure with Penalty for intermediate materials, Bendsøe & Sigmund, 1999), the design space includes a continuous variation of material between solid ($\rho = 1$) and void ($\rho = 0$). The constitutive behavior depends on the relative density ρ and the solid material elasticity tensor $\mathbf{D}$ through the following expression:

$$\mathbf{D}_\rho = f_D\left(\rho\right)\mathbf{D} = \rho^p\mathbf{D}, \tag{3}$$

$$\sigma = \mathbf{D}_\rho\varepsilon \ . \tag{4}$$

The effective stress tensor $\bar{\sigma}$ for an arbitrary intermediate material is set to be greater than the homogenized stress σ and dependent on the original (solid material) elasticity tensor and on the apparent (homogenized) value of deformation (Duysinx & Bendsøe ,1998):

$$\bar{\sigma} = \mathbf{D}\,\varepsilon \ . \tag{5}$$

For a given effective stress tensor $\bar{\sigma}$ an equivalent scalar stress σ_e (for example, von Mises) is computed. With this value, a failure function is defined as

$$F\left(\bar{\sigma}\right) = \frac{\sigma_e}{\sigma_{adm}} - 1 \leq 0, \tag{6}$$

where σ_{adm} is the material yielding stress or admissible maximum value. When density goes to zero, high deformations may occur due to low stiffness and consequently, large but finite local effective stresses are computed. This phenomenon, known as *Stress Singularity*, is characterized for introducing a discontinuity on the failure function for null values of ρ.The ϵ-regularization technique proposed by Cheng & Guo (1997) is used to overcome this inconvenience through the following re-definition of the failure function:

$$\begin{cases} g(\mathbf{x}) \equiv \rho(\mathbf{x}) F(\bar{\sigma}(\mathbf{x})) - \epsilon(1-\rho(\mathbf{x})) \leq 0, & a.e.\ in\ \Omega\ , \\ 0 < \epsilon^2 = \rho_{\min} \leq \rho(\mathbf{x}) \leq 1, & \forall\ \mathbf{x} \in \Omega. \end{cases} \tag{7}$$

The optimization problem is then set as the minimization of the functional $m(\rho)$ subject to a set of local failure constraints:

$$\underset{\rho \in W_{\rho}^{1,2}(\Omega)}{\text{Min}}\ m(\rho) = \int_{\Omega} \rho\, d\Omega + \frac{1}{2} r_{\rho} \int_{\Omega} f_{\rho}(\rho)\ d\Omega + r_m \int_{\Omega} f_m(\rho)\ d\Omega \tag{8}$$

$$Subject\ to: g_i(\mathbf{x}) \leq 0 \quad a.e.\ in\ \Omega, \quad i = 1...N,$$

where

$$\begin{aligned} f_{\rho}(\rho) &= (\nabla\rho)^T (\nabla\rho)\ , \\ f_m(\rho) &= \rho(1-\rho)\ , \\ W_{\rho}^{1,2}(\Omega) &= \left\{ \rho \mid \rho \in W^{1,2}(\Omega);\ 0 < \rho_{\min} \leq \rho(\mathbf{x}) \leq 1\ \forall\ \mathbf{x} \in \Omega \right\} \end{aligned}$$

The checker-board phenomenon is controlled by the second term of $m(\rho)$, which is a penalization of the density gradients (Pereira (2001), Pereira et all (2001), Borrvall (2001)). The third term introduces an explicit penalization of the intermediate densities. Constants r_m and r_{ρ} are the corresponding penalization factors.

Aiming to obtain numerical solutions, a classic Augmented Lagrangian functional is defined by introducing the stress constraints as penalization terms into the cost function:

$$\pounds(\rho; \lambda, \mathbf{r}) = m(\rho) + \sum_{i=1}^{N} m_i(\rho; \lambda_i, r_i) = m(\rho) + \sum_{i=1}^{N} \int_{\Omega} M_i(\rho; \lambda_i, r_i)\, d\Omega, \tag{9}$$

$$M_i(\rho; \lambda_i, r_i)\, d\Omega = \frac{1}{r_i} \max \left\{ g_i(\rho, \bar{\sigma}_i) \left[\lambda_i r_i + \frac{1}{2} g_i(\rho, \bar{\sigma}_i) \right] ; -\frac{(r_i \lambda_i)^2}{2} \right\}. \tag{10}$$

The penalization functional $m_i(\rho; \lambda_i, r_i)$ for the i-th load case consist of linear and quadratic terms of the failure function g_i that are multiplied by a penalization parameter $r_i > 0$ and by a Lagrangian function $\lambda_i \in L^2(\Omega)$. Thus, for a given set $\mathbf{r}^k = \{r_1^k, r_2^k, ..., r_N^k\} > 0$ and $\lambda^k = \{\lambda_1^k, \lambda_2^k, ..., \lambda_N^k\}$, $\lambda_i^k, \in L^2(\Omega)$, the following box-constrained problem can be solved:

$$\underset{\rho \in W_{\rho}^{1,2}(\Omega)}{\text{Min}}\ \pounds\left(\rho; \lambda^k, \mathbf{r}^k\right) \tag{11}$$

The solution of the whole optimization problem is obtained by solving a sequence of subproblems (11) with an adequate updating of parameters $\lambda^k, \mathbf{r}^k$. In this work the standard Augmented Lagrangian updating rule was chosen (Bertsekas, 1996):

$$\lambda_i^{k+1} = \max \left\{ \lambda_i^k + \frac{1}{2} g_i(\rho, \bar{\sigma}_i); 0 \right\}, \quad r_i^{k+1} = \frac{r_i^{k+1}}{t}, \quad t > 1\ . \tag{12}$$

3 Sensitivity Analysis

The algorithm chosen to solve problem (11) needs information of first order derivatives of the Lagrangian functional. Detailed operations to obtain analytical expressions of these gradients are found in Pereira et all (2003). The directional (Gateaux) derivative of the objective functional $\pounds\left(\rho; \lambda^k, \mathbf{r}^k\right)$ for fixed and known values of λ^k and $\mathbf{r}^k$ is given by:

$$\dot{\pounds}\left(\rho; \lambda^k, \mathbf{r}^k\right)[y] = \dot{m}(\rho)[y] + \sum_{i=1}^{N} \dot{m}_i\left(\rho; \lambda_i^k, r_i^k\right)[y], \tag{13}$$

$$\dot{m}(\rho)[y] = \int_{\Omega} \left[1 + r_m \frac{df_m(\rho)}{d\rho} + \frac{1}{2} r_{\rho} \frac{df_{\rho}(\rho)}{d\rho} \right] y\, d\Omega, \tag{14}$$

$$\dot{m}_i\left(\rho; \lambda_i^k, r_i^k\right)[y] = m_i'\left(\rho; \lambda_i^k, r_i^k\right)[y] - B'(\mathbf{u}_i, \mathbf{u}_i^a)[y] + l'(\mathbf{u}_i^a)[y]\ , \tag{15}$$

$$m_i'\left(\rho;\lambda_i^k,r_i^k\right)[y]=\int_\Omega \frac{\partial M_\sigma\left(\rho;\lambda_i^k,r_i^k\right)}{\partial\rho}\, y\, d\Omega\,,$$
$$=\int_\Omega \left\{\frac{1}{r_i^k}\left[F\left(\sigma_i\right)+\epsilon\right]\left\langle g_i\left(\rho,\bar{\sigma}_{\mathbf{i}}\right)+r_i^k\lambda_i^k\right\rangle^+\right\}\, y\, d\Omega\,. \tag{16}$$

In these expressions, y is a variation of ρ, $\mathbf{u}_i$ is the displacement field for the i-th load case and $\mathbf{u}_i^a$ is the adjoint solution for the i-th adjoint problem associated to the corresponding load case. The first term, $m(\rho)$, depends explicitly on density ρ and its derivative is straightforward. The penalization terms $m_i\left(\rho;\lambda_i^k,r_i^k\right)$ are implicitly dependent on ρ through the mechanical solutions $\mathbf{u}_i\left(\rho\right)$ for each load case. Their derivatives are obtained by the adjoint method (Haug et all, 1986). The partial (Gateaux) derivative of B for fixed real displacements $\mathbf{u}_i$ and adjoint solution $\mathbf{u}_i^a$ is given by

$$B'\left(\mathbf{u}_i,\mathbf{u}_i^a\right)[y]=\lim_{s\to 0}\left[\frac{B_{\rho+sy}\left(\mathbf{u}_i,\mathbf{u}_i^a\right)-B_\rho\left(\mathbf{u}_i,\mathbf{u}_i^a\right)}{s}\right]$$
$$=\int_\Omega q\rho^{(q-1)}\left[\mathbf{D}\nabla^S\mathbf{u}_i\cdot\nabla^S\mathbf{u}_i^a\right]\, y\, d\Omega\,. \tag{17}$$

Moreover, it is assumed (for simplicity sake) that external loads do not depend on ρ and then $l_i'\left(\mathbf{u}_i^a\right)[y]=0$. The solution $\mathbf{u}_i^a$ is computed from classical expression of the adjoint problem:

$$B\left(\mathbf{u}_i^a,\mathbf{v}\right)=\int_\Omega\left(\frac{\partial M_i}{\partial\nabla^S\mathbf{u}}\cdot\nabla^S\mathbf{v}\right)d\Omega\,,\quad\forall\ \mathbf{v}\in V, \tag{18}$$
$$=\int_\Omega\left(\frac{\rho}{r_i^k}\left\langle g_i\left(\mathbf{x}\right)+r_i^k\lambda_i^k\right\rangle^+H^{\sigma i}\cdot\nabla^S\mathbf{v}\right)d\Omega\,,\quad\forall\ \mathbf{v}\in V, \tag{19}$$

where $H^{\sigma i}$ is a second order tensor obtained explicitly from the material failure criterion evaluated at the current stress state $\sigma_i=\sigma(\mathbf{u}_i)$.

It is important to make some comments on the computational cost of these computations. To evaluate the Lagrangian functional $\pounds$ for given values of $\rho,\lambda^k,\mathbf{r}^k$, a set of N equilibrium solutions $\mathbf{u}_i$ are needed. To obtain the gradient of $\pounds$, the additional computation of N adjoint solutions $\mathbf{u}_i^a$ (plus some integration effort) is also required. Moreover, the bilinear form $B_\rho\left(\cdot,\cdot\right)$ for the adjoint problem and for real problem is the same and it is independent on the load condition. If essential boundary conditions do not change with loads, the computation $\mathbf{u}_i$, $\mathbf{u}_i^a$, $i=1...N$, may be performed with the same triangularized stiffness matrix and with N back-substitutions. Thus, the effort spent to calculate the value of the cost function is practically the same as that to compute the gradient of it.

4 Discretization and numerical procedure

Present implementation is limited to 2D problems although the formulation applies for 3D problems as well. Due to their flexibility in mesh generation and low computational costs, the classical three-node Lagrangian element was used to solve the boundary value problem. The same shape functions are used to define a continuous density field ρ whose nodal values play the role of design variables. Checkerboard phenomenon, common in low-order elements, is easily stabilized with the penalization term on density gradient. Failure function is evaluated at element level at the element centroid. Thus, the number of design variables is proportional to the number of nodes while the number of stress constraints is proportional to the number of elements (which in triangular meshes is approximately twice the number of nodes)

As proposed in Section 2, the Augmented Lagrangian procedure is used which implies the solution of a sequence minimization subproblems. For the k-th subproblem a set of Lagrangian multipliers and penalization factors $(\lambda^k,\mathbf{r}^k)$ is set and the minimization of the objective functional $\pounds(\rho;\lambda^k,\mathbf{r}^k)$ subject to side constraints is performed. This sequence follows the next strategy:

1. Define $k=0$, r_m, r_ρ, λ^k and $\mathbf{r}^k$;
2. Minimize the functional $\pounds\left(\rho;\lambda^k,\mathbf{r}^k\right)$, $0<\rho_{\min}\leq\rho\left(\mathbf{x}\right)\leq 1$;
3. Verify convergency within a tolerance. If satisfied, stop the process;
4. Update η^k, λ^k, $\mathbf{r}^k$;
5. $k=k+1$, Return to Step 2.

The optimization algorithm used in Step 2 is a non-linear trust-region algorithm proposed by Friedlander et all, 1994 . This algorithm was generalized by Bielschowsky et all, 1997, and it is based on the construction of a quadratic subproblem defined on a trust region and on the search algorithm along its sides. An adaptive strategy is also used based on the quality of the approximated subproblem that modifies the size of the trust region to accelerate convergence. The results ot this work were obtained with an implementation of this algorithm, called BOX-QUACAN, provided by the former authors and parametrically adapted to the present case.

5 Numerical Results

This section is devoted to show some results comparing optimal designs due to different load cases and due to their combination. An analysis of the influence of the set of parameters like $r_m, r_\rho, \lambda^k, \mathbf{r}^k$ and ϵ on numerical results is found in Pereira et all (2003). In present examples the following values were used, unless a difference is particularly specified: $r_m = 0,95$, $r_\rho = 0.001$, $\mathbf{D} = \rho^3\mathbf{D}$, $\epsilon^2 = \rho_{\min} = 0.01$.

5.1 Traction and bending of a beam

This simple example exploites many particularities of the present formulation and points out some polemic aspects such as the fully stressed design condition. Analogous example was shown in Pereira (2003) but no multiple loaded case was analyzed. The background domain is a square beam with symmetry boundary conditions on the left side and submitted to traction and bending forces on the right side (see Figure 2). The value of $t_t = 17.5\ Pa$ while $t_b = 30\ Pa$. The stress limit is $\sigma_{adm} = 35Pa$. Other parameters are $E = 100Pa$, $\nu = 0.3$. Two regions are defined; the left one is submitted to optimization while the right one is fixed. Figure 3 show the final design for the first load case in which a bar of half the transversal section of the original bar is obtained. A fully stressed design condition is fulfilled on the left side of the bar while a smooth, not fully-stressed transition is found on the right side. Different design is obtained for the "pure-bending" case (Figure 4). Material is spread up and down in order to increase the moment of inertia of the cross section. The failure function is saturated only at the extreme lower and upper boundaries, what show a didactic case in which a fully-stressed design condition cannot be achieved: further elimination of material even in a non saturated region will produce inadmissible stress values at upper/lower boundaries of the beam. The consideration of both (not simultaneous) loads is shown in Figure (5) It is possible to see that the cross section maintains half the size of the original one in order to support traction forces. Two bars remain at the "flanges" of the beam but a different transition with the fixed part of the beam was obtained. Moreover, as traction can bend the "flanges", a thin vertical column is inserted to avoid this movement. Figures 6 and 7 show the ϵ-relaxed failure function of this final design for each of both load cases

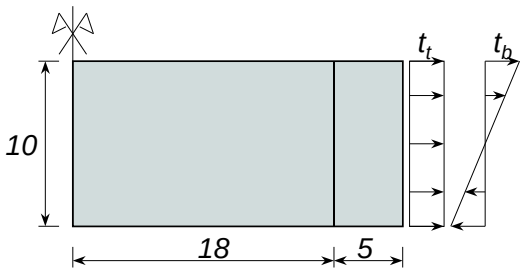

Figure 2: Traction and bending of beam.

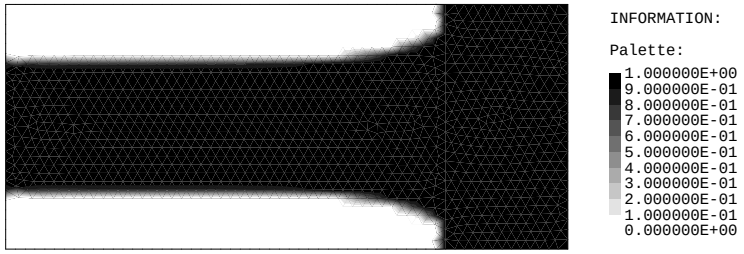

Figure 3: Density distribution for traction load.

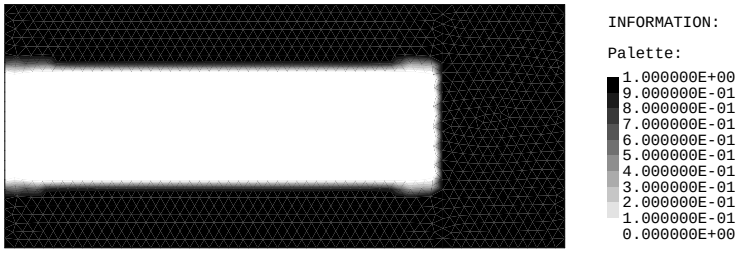

Figure 4: Density distribution for bending load.

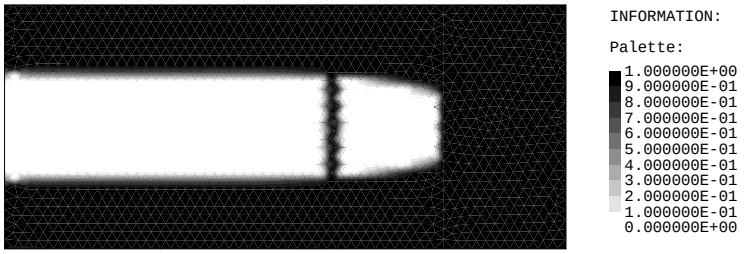

Figure 5: Density distribution for traction and flexion loads.

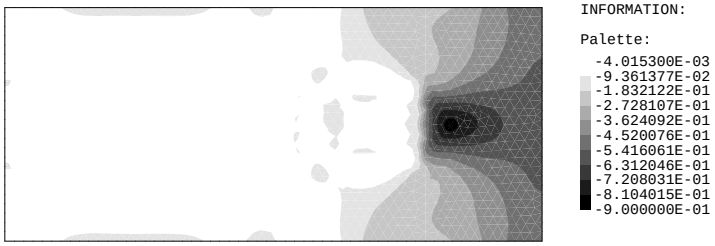

Figure 6: Multiple load case design. ϵ-relaxed failure function for traction load.

5.2 Anisotropic failure criterion

This example shows a case in which the failure function behaves different in traction than in compression. The failure function is defined by the model of Raghava (Raghava et all, 1973) and the example consists in a squared background mesh submitted to a distributed force applied to a small region at bottom with fixed density (see Figure 8). The upper boundary is clamped. The same load is applied to up, down, left and right directions. The value of the total force is $P_1 = P_2 = P_3 = P_4 = 1N$. The admissible stress in traction is $\sigma^t_{adm} = 2.5\,Pa$ and in compression $\sigma^c_{adm} = 7.5\,Pa$. Material parameters are $E = 100\,Pa$, $\nu = 0.3$, $L = 1m$. Figure 9 show the final design for Load 1. As expected, the bar in traction has a wider cross section. Similar behavior happens for the third and fourth loads at vertical direction. Figures 10 show the final design for Load 3 (traction). The final density distribution due to the four loads individually applied is presented in Figure 11. It is possible to see that this topology and shape is quite similar to that of the first load but with both bars with the same height, which is clearly a consequence of failure constraints to loads 1 and 2. The ϵ-relaxed failure function of this final design for loads 1 and 3 are shown in Figures 12,13.

5.3 Constrained domain

This example can be classified as belonging to those cases in which the background domain introduces an initial geometric constraint. This type of problems is perhaps the most usual case in practical applications: the final design must fit in an available room.

Due to the existence of a singular stress point at the inner corner of the L-shaped initial background domain, the present case may be used as a benchmark for those formulations that search the satisfaction of failure constraints; the algorithm should find a final shape avoiding these inial stress concentrations. Two load are applied on a small fixed region at the right side of the initial domain (see Figure 14). The solution for the vertical load was considered in Pereira et all (2003) and it is shown in Figure 15a). Material and geometric data is $E = 100Pa$, $\nu = 0.3$, $L = 1.0m$, $\sigma_{adm} = 42.42\,Pa$, $P_1 = P_2 = 1.0N$. The final design for the horizontal load and for the multiple load condition are shown in figures 15b),16. Comparing the solution due to the vertical load with that for the multiple loaded case it is possible to see the accentuation of the radius close to the inner initial corner as well as the the

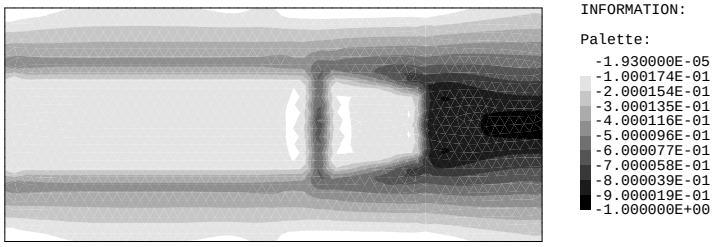

Figure 7: Multiple load case design. ϵ-relaxed failure function for flexion load.

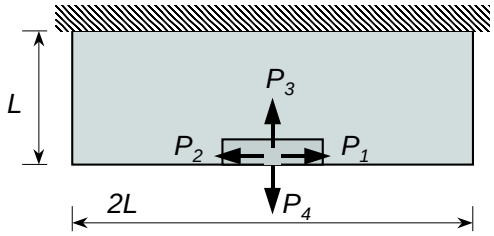

Figure 8: Anisotropic failure function.

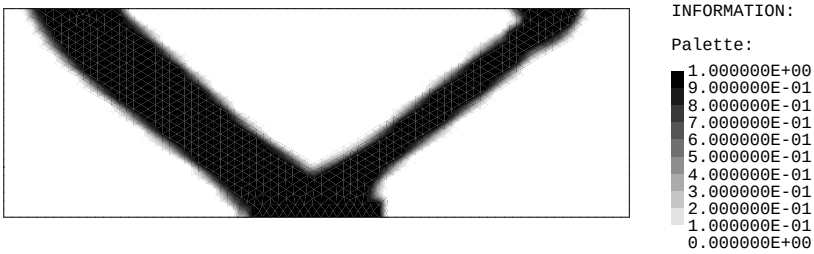

Figure 9: Density distribution for load 1.

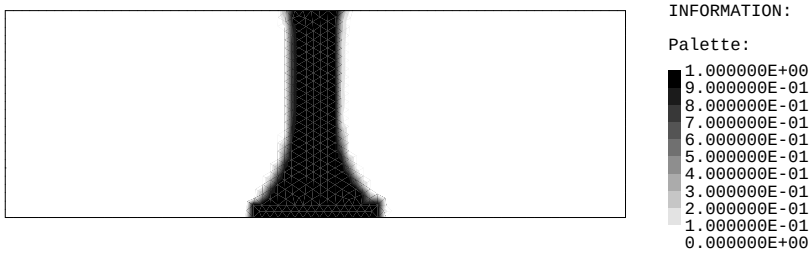

Figure 10: Density distribution for load 4.

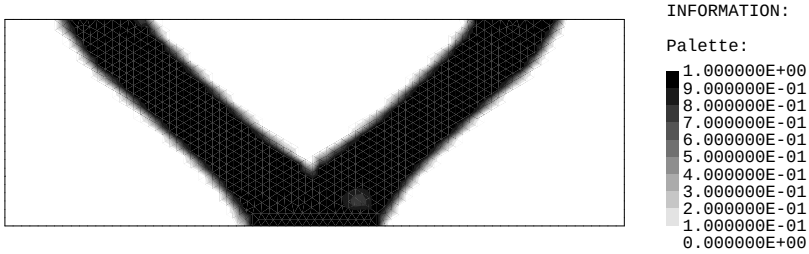

Figure 11: Density distribution for multiple load conditions (loads 1 to 4).

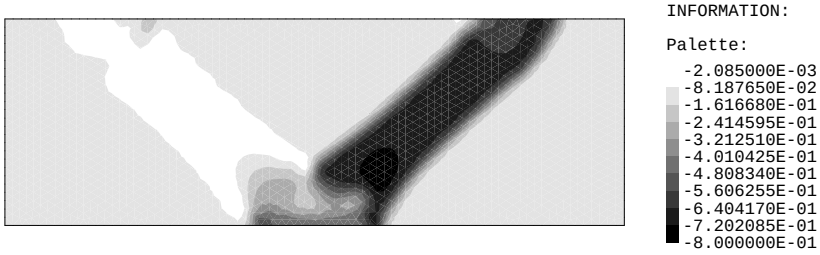

Figure 12: Multiple load case. ϵ-relaxed failure function for load 1.

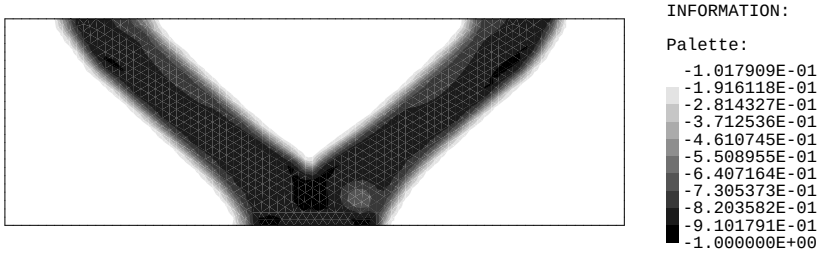

Figure 13: Multiple load case. ϵ-relaxed failure function for load 4.

growth of the cross section near the clamped boundary due to bending stresses produced by the horizontal load.

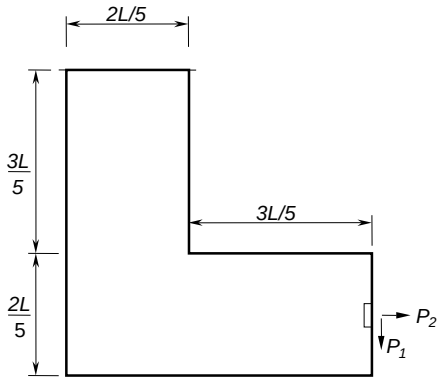

Figure 14: Constrained domain.

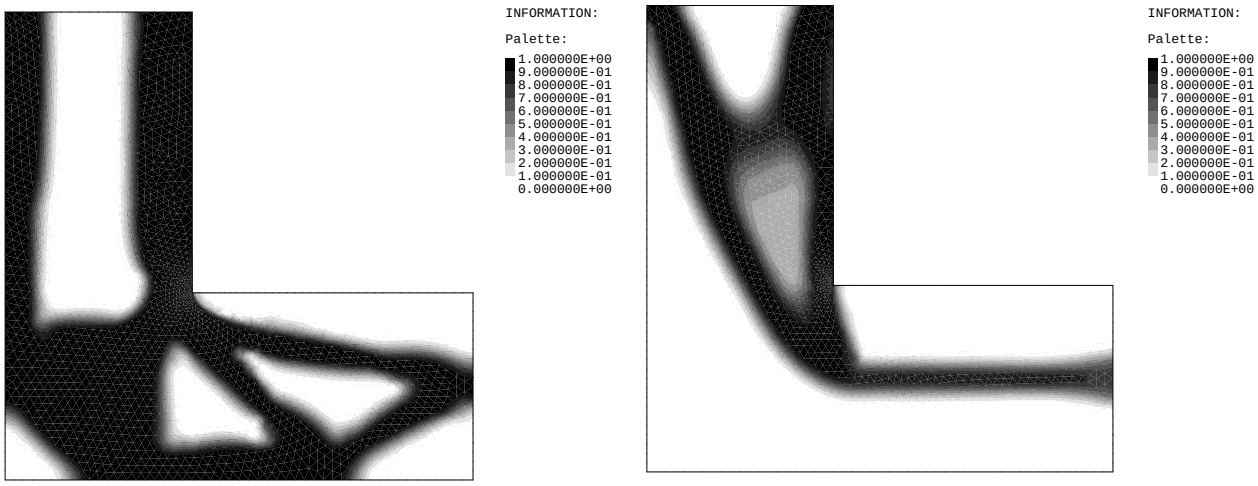

Figure 15: Density distribution for a)vertical load and b)horizontal load.

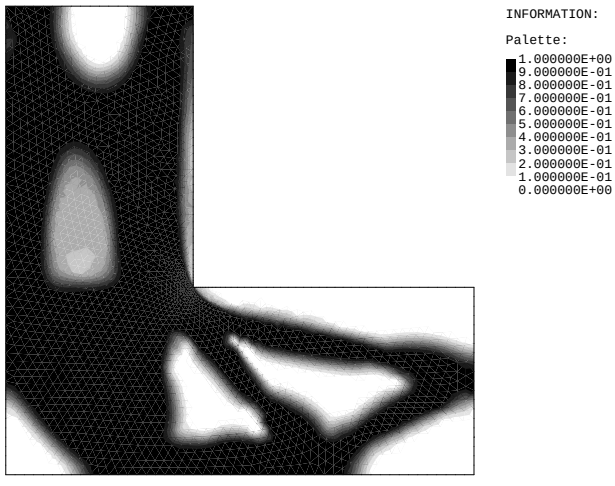

Figure 16: Density distribution for vertical and horizontal loads.

6 Final considerations

This work discusses the consideration of a multiple load cases in a formulation oriented to minimize the mass of a mechanical component subject to material failure constraints. The theoretical principles of the problem are briefly outlined and follow the same formulation shown in Pereira (2001) and Pereira et all (2003) for a single loaded problem. The numerical results show, as expected, significative differences of design for each load. Moreover, the final design that satisfies failure constraints for all individual loads shows a topology that is not just an "envelope" of each individual design (which is the most frequent intuitive guess). From a numerical point of view, it is claimed that, for the present formulation, the computational effort spent to consider failure constraints due to multiple loads is not much grater than for that for a single loaded case; if the same essential boundary conditions are considered, the same triangularized stiffness matrix is used for each load and, consequently, multiple solutions and adjoint solutions for gradient computations are easily performed by back-substitution operations. Unfortunately, real problems submitted to different loads usually produces different contact regions and load transmission in mechanical devices. The consideration of contact conditions in multiple loaded is object of future works.

7 Acnowledgments

The authors are grateful to Ana Friedlander, Sandra A. Santos and José M. Martínez (IMECC/UNICAMP) for the use of the algorithm BOX-QUACAN. We thank also to the group TACSOM (*Theoretical, Applied and Computational Solid Mechanics Group)* (www.lncc.br/~tacsom) for the computational facilities of the system ACDPOOP/ACDPFEM. This work is partially supported by CNPq, project number 551549/2002-5.

References

[1] M.P. Bendsøe and O. Sigmund. Material interpolation schemes in topology optimization. *Archive of Applied Mechanics*, 69:635–654, 1999.

[2] D.P. Bertsekas. *Constrained Optimization and Lagrange Multiplier Methods.* Athena Scientific, Belmont, MA, EUA, 1996.

[3] R.H. Bielschowsky, A. Friedlander, F.A.M. Gomes, J.M. Martínez, and M. Raydan. An adaptive algorithm for bound constrained quadratic minimization. *Investigación Operativa*, 7:67–102, 1997.

[4] T. Borrvall. Topology optimization of elastic continua using restriction. *Archives on Computational Methods in Engineering*, 190:4911–4928, 2001.

[5] G.D. Cheng and X. Guo. ε–Relaxed approach in structural topology optimization. *Structural Optimization*, 13:258–266, 1997.

[6] J.E. Sousa de Cursi and E. Pagnaco. Minimun mass parts in 2D elasticity. pages 231–236, Goslar, Germany, June 1995. Pergamon Press Ltd.

[7] P. Duysinx and M.P. Bendsøe. Topology optimization of continuum structures with local stress constraints. *International Journal for Numerical Methods in Engineering*, 43:1453–1478, 1998.

[8] P. Duysinx and O. Sigmund. New developments in handling stress constraints in optimal material distribution. In *7th AIAA/USAF/NASA/ISSMO Symposium on Multidisciplinary Design Optimization*, pages 98/4906/1–9, Saint Louis, MI, EUA, 1998. American Institute of Aeronautics and Astronautics.

[9] A. Friedlander, J.M. Martínez, and S.A. Santos. A new trust-region algorithm for bound constrained minimization. *Applied Mathematics and Optimization*, 30(3):235–266, 1994.

[10] E.J. Haug, K.K. Choi, and P.V. Komkov. *Design Sensitivity Analysis of Structural Systems.* Academic Press, Orlando, FL, EUA, 1986.

[11] S. Idelsohn, E. Oñate, and E. Dvorkin, editors. *WCCM IV – Proceedings of the Fourth World Congress on Computational Mechanics*, Buenos Aires, Argentina, June 1998. Centro Internacional de Métodos Numéricos en Ingeniería.

[12] C.-Y. Lin and L.-S. Chao. Constant-weight fully stressed methods for topological design of continuum structures. *Computer Methods in Applied Mechanics and Engineering*, 190:6867–6879, 2001.

[13] A.A. Novotny, E.A. Fancello, and J.E. Souza de Cursi. An h adaptive topological optimization design in 2D elasticity. In Idelsohn et al. [11].

[14] J. T. Pereira. *Otimização Topológica de Componentes Mecânicos com Restrições sobre o Critério de Falha Material.* Ph.d. thesis, GRANTE – Grupo de Análise e Projeto Mecânico – Departamento de Engenharia Mecânica – Universidade Federal de Santa Catarina, Florianópolis, SC, Brasil, 2001.

[15] J. T. Pereira, E.A. Fancello, and C. S. Barcellos. Sobre o controle de checkerboard em otimização topológica estrutural. In *CILAMCE 2001 – Proceedings of the Iberian Latin–American Congress on Computational Methods in Engineering*, São Paulo, Brasil, November 2001.

[16] J. T. Pereira, E.A. Fancello, and C. S. Barcellos. Topology optimization of continuum structures with material failure constraints. *Structural and Multidisciplinary Optimization*, (to be published), 2003.

[17] O.M. Querin, G.P. Steven, and Y.M. Xie. Evolutionary structural optimization using additive algorithm. *Finite Elements in Analysis and Design*, 34:291–308, 2000.

[18] R. Raghava, R.M. Caddell, and G.S.Y. Yeh. The macroscopic yield behaviour of polymers. *Journal of Materials Science*, 8:225–232, 1973.

[19] M. Stolpe and K. Svanberg. Modelling topology optimization problems as mixed 0-1 programs. Internal Report KTH/OPT SYST/FR 01/10 SE, KTH – Optimization and Systems Theory – Department of Mathematics – Royal Institute of Technology, Stockholm, Suécia, October 2001.

[20] Y.M. Xie and G.P. Steven. A simple evolutionary procedurefor structural optimization. *Computers and Structures*, 49(5):885–969, 1993.

[21] Y.M. Xie and G.P. Steven. *Evolutionary structural optimization.* Springer, London, 1997.